

Learning to Generate Time-Lapse Videos Using Multi-Stage Dynamic Generative Adversarial Networks

Wei Xiong*, Wenhan Luo[†], Lin Ma[†], Wei Liu[†], and Jiebo Luo*

*Department of Computer Science, University of Rochester, Rochester, NY 14623

[†]Tencent AI Lab, Shenzhen, China

{wxiongwhu, forest.linma, jiebo.luo}@gmail.com, wenhanluo@tencent.com, wliu@ee.columbia.edu

Abstract—Taking a photo outside, can we predict the immediate future, like how the cloud would move in the sky? We answer this question by presenting a generative adversarial network (GAN) based two-stage approach to generating realistic time-lapse videos of high resolution. Given the first frame, our model learns to generate long-term future frames. The first stage aims to generate videos of similar content as that in the input frame and of plausible motion dynamics. The second stage refines the generated video from the first stage by enforcing it to be closer to real videos with regard to dynamics. To further encourage realistic motion in the final generated video, Gram matrix is employed to model the motion more precisely. We build a large scale time-lapse dataset, and test our approach on this new dataset. Using our model, we are able to generate up to 128×128 resolution videos for 32 frames in a single forward pass. Quantitative and qualitative experiment results demonstrate the superiority of our method over the state-of-the-art methods.

I. INTRODUCTION

Humans can often estimate fairly well what will happen in the immediate future given the current scene. However, for vision systems, predicting the future states is still a challenging task. The problem of future prediction or video synthesis has drawn more and more attention in recent years since it is critical for various kinds of vision applications, such as automatic driving, video understanding [1], and robotics [2]. The goal of video prediction in this paper is to generate plausible, long-term, and high-quality future frames given one starting frame. Achieving such a goal is difficult, as it is challenging to model the multi-modality and uncertainty in generating both the content and motion in future frames.

For the content generation, the main problem is what to learn. Generating future on the basis of only one static image encounters inherent uncertainty of the future, which has been illustrated in [3]. Since there can be multiple possibilities for reasonable future scenes following the first frame, the objective function is difficult to define. Generating future frames by simply learning to reconstruct the real video can lead to unrealistic results [4] and [5]. Several models including [6] and [4] are proposed to address this problem based on generative adversarial networks. For example, 3D convolution is incorporated in an adversarial network to

model the transformation from an image to video in [4]. Their model produces plausible futures given the first frame. However, as the model updates, the generated video tends to be blurry and lose content details, which degrades the realism of the generated videos. A possible cause is that the encoder-decoder structure in the generator fails to preserve all the indispensable details of the content.

In terms of motion transformation, the main challenge is to drive the given frame to transform realistically over time. Some prior works have investigated this problem. Zhou and Berg [7] use a RNN to model the temporal transformations. They are able to generate a few types of motion patterns, but not realistic enough. It may be due to the fact that, each future frame is based on the state of the previous frames, so the error could accumulate and the motion could distort over time. The information loss and error accumulation during the long-term image sequence generation hinder the success of video prediction.

We dive into both content and motion modeling and propose a Multi-stage Dynamic Generative Adversarial Network (MD-GAN) to improve the performance in future prediction. Specifically, there are two stages in the proposed approach. The first stage handles content generation and the second stage specifically deals with motion modeling.

To be more specific, we adopt the idea in [4] and develop a generative adversarial network called Base-Net to generate contents in the first stage. The adversarial loss of this GAN framework encourages the generator to produce videos that are of the similar distributions as the real ones. Unlike [4], we use a U-net like architecture in the generator instead of the vanilla encoder-decoder structure in order to better preserve content details in the videos. We use the identity skip connections [8] to link feature maps in the encoder and decoder. The decoder of the generator then leverages previous features in the encoder, thus reducing the information loss. In this way, the model is able to generate plausible future frames, which are visually more pleasing than the counterpart.

To generate more realistic future frames with vivid motion, the second stage of the proposed MD-GAN takes the output of the first stage as input, and refines it with another generative adversarial network, which we call Refine-Net.

We propose an adversarial ranking loss to train the network so as to encourage the generated video to be closer to the real one while further away from the input video (from stage I) regarding motion. To this end, we introduce the Gram matrix [9] to model the dynamic transformations among consecutive frames.

To evaluate the proposed model, we build a large scale time-lapse video dataset called Sky Scene. This dataset includes daytime, nightfall, starry sky, and aurora scenes. We train our model on this dataset and then predict the future frames given a static picture of sky scene. We are able to produce 128×128 realistic videos, whose resolution is much higher than those of the state-of-the-art models. Note that, unlike some prior works which generate merely one frame at a time, our model generates 32 future frames by a single pass, further preventing error accumulation and information loss.

Our key contributions are as follows:

- 1) We build a large scale time-lapse video dataset, which contains high-resolution dynamic videos of the sky scenes.
- 2) We propose a Multi-stage Dynamic Generative Adversarial Network (MD-GAN), which can effectively capture the spatial and temporal transformations in an adversarial manner, thus generating realistic time-lapse future frames given only one starting frame.
- 3) We introduce the Gram matrix for motion modeling and propose an adversarial ranking loss to mimic motions of real-world videos, which refines our preliminary outputs in the first stage and produces more realistic and higher-quality future frames.

II. RELATED WORK

A. Generative Adversarial Networks

Our multi-stage model takes advantages of generative adversarial networks (GAN) [10]. A generative adversarial network is composed of two parts, a generator and a discriminator. The generator tries to fool the discriminator by producing samples similar to real ones, while the discriminator is trained to distinguish the generated samples from the real ones. The two models are trained in an adversarial way and finally they can reach a “Nash Equilibrium”. GAN has been successfully applied to the task of image generation. For example, in the seminal paper [10], models trained on the MNIST dataset and the Toronto Face Database (TFD), respectively, generate images of digits and faces with high likelihood. Relying only on random noise, the original GAN cannot control the mode of the generated samples. To solve this problem, conditional GAN [11] is proposed. Images of digits conditioned on class labels and captions conditioned on image features are generated. Many subsequent works are variants of conditional GAN. Convolutional Neural Network (CNN) has also been adopted in [12] to train GAN.

Proposing a set of architectural guidelines, the authors obtain a stable deep convolutional GAN. In [13], the Wasserstein distance is introduced to stabilize the training of GAN. The tasks of image-to-image translation and text-to-image translation, have also employed GAN. Pix2pix [14], CycleGAN [15] and [16] are representative examples. Inspired by the coarse-to-fine strategy, multi-stack methods such as [17, 18] have been proposed to first generate low-resolution images and then refine them to higher-resolution images with finer details.

B. Video Generation

The task of video generation or future prediction has drawn more and more research attention in recent years. Based on conditional variational auto-encoder [19], Xue et al. [20] propose a cross convolutional network to model layered motion, which applies learned kernels to image features encoded in a multi-scale image encoder. The output is a difference image, which can be added to the current frame to produce the next frame. Since the inception of GAN, there are many approaches employing GAN for the task of future prediction. In [4], an independent two-stream convolutional neural network, one for foreground and the other one for background, is proposed for video generation from noise. Combining the dynamic foreground stream and the static background stream, the generated video looks real. In the follow-up work [3], Vondrick and Torralba formulate the future prediction task as transforming pixels in the past to future. Based on large scale unlabeled video data, a CNN model is trained with adversarial learning as a transformer for this task. Content and motion are decomposed and encoded separately by multi-scale residual blocks, and then combined and decoded to generate future video frames in [21]. Plausible results are achieved on both the KTH dataset and the Weizmann dataset. A similar idea is presented in [22]. To generate long-term future frames, Villegas et al. [6] do not directly generate future frames. Instead, they estimate high-level structure (human body pose in their case), and learn LSTM and analogy-based encoder-decoder convolutional neural networks to generate future frames based on the current image and the estimated high-level structure.

The closest work to ours is [7], which also generates time-lapse videos based on GAN. However, there are a few important differences between their work and ours. First, our method is based on 3D convolution while Zhou and Berg [7] employ a recurrent neural network to recursively generate future depictions, which is prone to error accumulation. Second, as modeling motion is indispensable for video generation, we explicitly model motion by introducing the Gram matrix. Finally, we generate high-resolution (up to 128×128) videos of dynamic scenes, while the generated videos in [7] are simple (usually with clean background) and of resolution 64×64 .

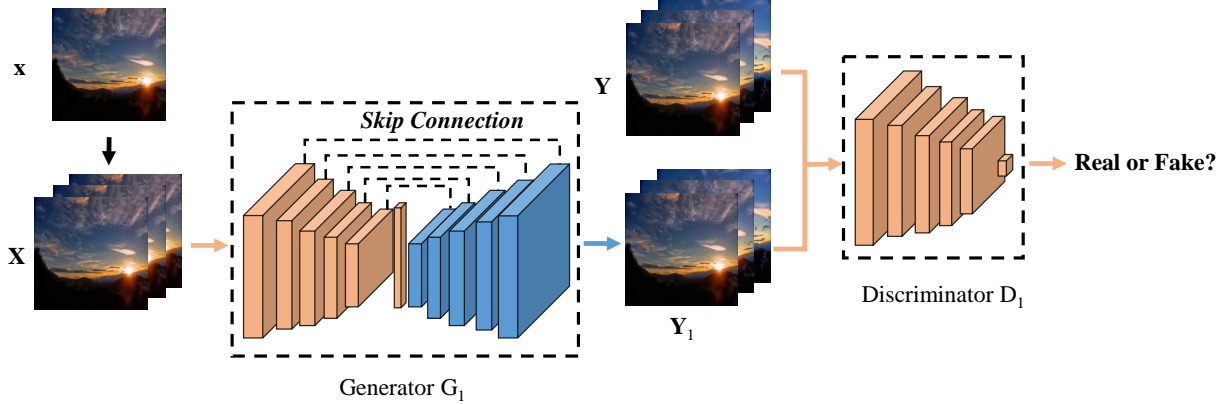


Figure 1. The structure of the Base-Net in Stage I. The input image is firstly duplicated to 32 frames as input to generator G_1 , which produces a fake video \mathbf{Y}_1 . The encoder of the generator is composed of 3D convolutional layers (the orange cubics), and the decoder is composed of 3D deconvolutional layers (the blue cubics). Intermediate layers of the encoder and the decoder are connected by skip connections. Discriminator D_1 then tries to distinguish the generated \mathbf{Y}_1 from the real video \mathbf{Y} .

III. OUR APPROACH

A. Overview

The proposed Multi-stage Dynamic GAN (MD-GAN) takes a single RGB image as input and attempts to predict the next few frames that are as plausible as possible with regard to real videos. Unlike the conventional models that directly output an image sequence, we instead use a multi-stage framework in a coarse-to-fine manner to progressively generate videos. Our model is composed of two stages. Given an input image \mathbf{x} , the model generates a video \mathbf{Y}_1 of T frames (including the input starting frame) in Stage I, which we call Base-Net. \mathbf{Y}_1 serves as a coarse estimation of the groundtruth \mathbf{Y} . Then in Stage II, our model takes \mathbf{Y}_1 as input, refines it with vivid motion dynamics by the Refine-Net, and produces a more vivid video \mathbf{Y}_2 as the final prediction.

B. Stage I: Base-Net

In general, the model of Stage I is a generative adversarial network, which is named as Base-Net. As shown in Fig. 1, the Base-Net is composed of a generator G_1 and a discriminator D_1 . Given an image $\mathbf{x} \in \mathbb{R}^{3 \times H \times W}$ as a starting frame, we duplicate it T times, obtaining a static video $\mathbf{X} \in \mathbb{R}^{3 \times T \times H \times W}$. \mathbf{X} serves as the input to generator G_1 . By forwarding \mathbf{X} through layers of 3D convolutions and 3D deconvolutions, the generator G_1 outputs a video $\mathbf{Y}_1 \in \mathbb{R}^{3 \times T \times H \times W}$ of T frames, i.e., $\mathbf{Y}_1 = G_1(\mathbf{X})$.

For generator G_1 , we adopt an encoder-decoder architecture, which is also employed in [12] and [4]. However, the vanilla encoder-decoder architecture encounters problems in generating decent results as the features from the encoder may not be fully exploited. Therefore, we utilize a 3D U-net like architecture [23] instead of the vanilla encoder-decoder architecture so that the rich features in the encoder can be fully made use of to generate \mathbf{Y}_1 . This may seem like a

small modification, yet it plays a key role in improving the quality of videos, as verified by the experiments.

The discriminator D_1 then takes video \mathbf{Y}_1 and the real video \mathbf{Y} as the input and tries to distinguish them. Note that \mathbf{x} is the first frame of \mathbf{Y} . D_1 shares the same architecture as the encoder part of G_1 , except that the final layer is a single node with a sigmoid activation layer.

To train our model, the adversarial loss of the network can be defined as:

$$\mathcal{L}_{adv} = \min_{G_1} \max_{D_1} \mathbb{E} [\log D_1(\mathbf{Y})] + \mathbb{E} [\log (1 - D_1(G_1(\mathbf{X})))] . \quad (1)$$

We also define a content loss function to ensure that the content of the generated video is similar to the content of the starting frame in the pixel space. As pointed out in [14], L_1 distance usually results in sharper outputs than L_2 distance. Thus, our content loss is defined as

$$\mathcal{L}_{con}(G_1) = \|\mathbf{Y} - G_1(\mathbf{X})\|_1 . \quad (2)$$

The final objective of our Base-Net in Stage I is

$$\mathcal{L}_{stage1} = \mathcal{L}_{adv} + \mathcal{L}_{con} . \quad (3)$$

Using the generative adversarial network, our Base-Net is able to generate plausible videos. The adversarial training allows our model to produce examples whose distribution overlaps with the real data distribution. However, as the learning capacity of the generative adversarial network is limited considering the uncertainty of the future, the model may not be able to capture most of the correct patterns existing in the real data. As a consequence, the generated videos might be plausible but not realistic enough. To tackle this problem, we further process the output from Stage I in Stage II by another network called Refine-Net, to

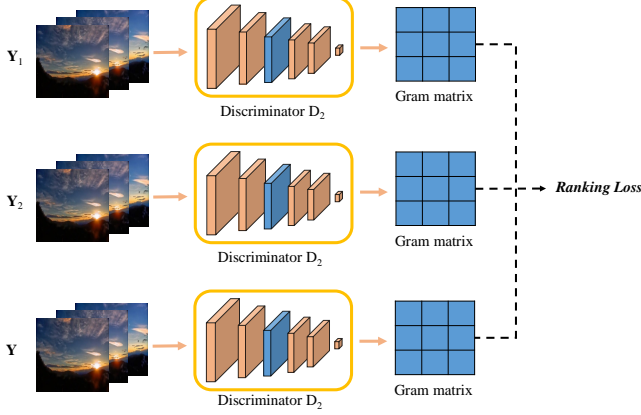


Figure 2. The adversarial ranking loss used in the Refine-Net. We firstly extract features of the input Y_1 , output Y_2 and the ground-truth video Y from the convolutional layer of D_2 , then use them to calculate a Gram matrix for each video. Following that, we calculate the adversarial ranking loss by measuring the distances between the Gram matrices.

compensate it for vivid motion dynamics and generate more realistic videos.

C. Stage II: Refine-Net

Inputting video Y_1 from Stage I, the Refine-Net improves quality of the generated video Y_2 to fool human eyes in telling which one is real against the groundtruth video Y . The idea of using multiple stages of GAN to generate finer results has also been employed in [17], which can be considered as a kind of content refinement. In contrast to their work, the purpose of our Refine-Net is to improve the quality of generated videos especially regarding *motion*.

The Refine-Net is similar to the Base-Net in Stage I, except that we remove a few skip connections in generator G_2 . However, naively employing this Refine-Net may lead to an identity mapping since the input Y_1 is an optimal result of such a structure, i.e. G_1 . As long as G_2 learns an identity mapping, the output Y_2 would not be improved. To prevent this from happening, we propose an adversarial ranking loss to drive the network to generate videos which are closer to real-world videos while further away from the input video (Y_1 from Stage I). The ranking loss is defined as $\mathcal{L}_{rank}(Y_1, Y, Y_2)$, which will be detailed later, with regard to the input Y_1 , output Y_2 and the ground-truth video Y . To construct such a ranking loss, we should take the advantage of effective features that can well represent the dynamics across frames. Based on such feature representations, distances between videos can be conveniently calculated.

We employ the Gram matrix [9] as the motion feature representation to assist G_2 to learn dynamics across video frames. Given an input video, we first extract features of the video with discriminator D_2 . Then the Gram matrix is calculated across the frames using these features such that it incorporates rich temporal information.

Specifically, given an input video Y , suppose that the output of the l -th convolutional layer in D_2 is $H_Y^l \in \mathbb{R}^{N \times C_l \times T_l \times H_l \times W_l}$, where (N, C_l, T_l, H_l, W_l) are the batch size, number of filters, the length of the time dimension, the height and the width of the feature maps, respectively. We reshape H_Y^l to $\hat{H}_Y^l \in \mathbb{R}^{N \times M_l \times S_l}$, where $M_l = C_l \times T_l$ and $S_l = H_l \times W_l$. Then we calculate the Gram matrix $g(Y; l)$ as follows:

$$g(Y; l) = \frac{1}{M_l \times S_l} \sum_{n=1}^N \hat{H}_Y^{l,n} (\hat{H}_Y^{l,n})^T, \quad (4)$$

where $\hat{H}_Y^{l,n}$ is the n -th sample of \hat{H}_Y^l . $g(Y; l)$ calculates the covariance matrix between the intermediate features of discriminator D_2 . Since the calculation incorporates information from different time steps, it can encode motion information of the given video Y .

The Gram matrix has been successfully applied to synthesizing dynamic textures in previous works [24, 25], but our work differs from them in several aspects. First, we use the Gram matrix for video prediction, while the prior works use it for dynamic texture synthesis. Second, we directly calculate the Gram matrix of videos based on the features of discriminator D_2 , which is updated in each iteration during training. In contrast, the prior works typically calculate it with a pre-trained VGG network [26], which is fixed during training. The motivation of such a different choice is that, as discriminator D_2 is closely related to the measurement of motion quality, it is better to directly use features in D_2 .

To make full use of the video representations, we adopt a variant of the contrastive loss introduced in [27] and [28] to compute the distance between videos. Our adversarial ranking loss with respect to features from the l -th layer is defined as:

$$\begin{aligned} \mathcal{L}_{rank}(Y_1, Y, Y_2; l) &= \frac{e^{-\|g(Y_2; l) - g(Y; l)\|_1}}{e^{-\|g(Y_2; l) - g(Y; l)\|_1} + e^{-\|g(Y_2; l) - g(Y_1; l)\|_1}} \\ &= -\log \frac{e^{-\|g(Y_2; l) - g(Y; l)\|_1}}{e^{-\|g(Y_2; l) - g(Y; l)\|_1} + e^{-\|g(Y_2; l) - g(Y_1; l)\|_1}}. \end{aligned} \quad (5)$$

Fig. 2 illustrates the procedure of calculating the proposed adversarial ranking loss. We extract the features of multiple convolutional layers in the discriminator, and calculate their Gram matrices individually. The final adversarial ranking loss is:

$$\mathcal{L}_{rank}(Y_1, Y, Y_2) = \sum_l \mathcal{L}_{rank}(Y_1, Y, Y_2; l). \quad (6)$$

Similar to the objective in Stage I, we also incorporate the pixel-wise L_1 distance to capture low-level details. The overall objective for the Refine-Net is:

$$\mathcal{L}_{stage2} = \mathcal{L}_{adv} + \lambda \cdot \mathcal{L}_{rank} + \mathcal{L}_{con}. \quad (7)$$

The generator and discriminator are trained alternatively. When training generator G_2 with discriminator D_2

Algorithm 1 Training procedure of the Refine-Net. When training the discriminator D_2 , we ascend the gradient of the adversarial ranking loss. When training the generator G_2 , we use gradient descent.

for number of iterations **do**

Sample N video clips $\{\mathbf{Y}^{(1)}, \dots, \mathbf{Y}^{(N)}\}$ from the training set.

Obtain the output of the Base-Net $\{\mathbf{Y}_1^{(1)}, \dots, \mathbf{Y}_1^{(N)}\}$.

Updating the discriminator D_2 by *ascending* the gradient:

$$\nabla_{\theta_d} \frac{1}{N} \sum_{n=1}^N \log D_2(\mathbf{Y}^{(n)}) + \log (1 - D_2(G_2(\mathbf{Y}_1^{(n)}))) + \lambda \cdot \mathcal{L}_{rank}(\mathbf{Y}_1^{(n)}, \mathbf{Y}^{(n)}, G_2(\mathbf{Y}_1^{(n)}))$$

Sample N new video clips $\{\mathbf{Y}^{(1)}, \dots, \mathbf{Y}^{(N)}\}$ from the training set.

Obtain the output of the Base-Net $\{\mathbf{Y}_1^{(1)}, \dots, \mathbf{Y}_1^{(N)}\}$.

Updating the generator G_2 by *descending* the gradient:

$$\nabla_{\theta_g} \frac{1}{N} \sum_{n=1}^N \log (1 - D_2(G_2(\mathbf{Y}_1^{(n)}))) + \lambda \cdot \mathcal{L}_{rank}(\mathbf{Y}_1^{(n)}, \mathbf{Y}^{(n)}, G_2(\mathbf{Y}_1^{(n)})) + \mathcal{L}_{con}$$

end for

fixed, we try to minimize the adversarial ranking loss $\mathcal{L}_{rank}(\mathbf{Y}_1, \mathbf{Y}, \mathbf{Y}_2)$, such that the distance between the generated \mathbf{Y}_2 and the groundtruth \mathbf{Y} is encouraged to be smaller, while the distance between \mathbf{Y}_2 and \mathbf{Y}_1 is encouraged to be larger. By doing so, the distribution of videos generated by the Refine-Net tends to be closer to that of the real ones, and the quality of videos from Stage I tends to be improved.

When training discriminator D_2 with generator G_2 fixed, on the contrary, we maximize the adversarial ranking loss $\mathcal{L}_{rank}(\mathbf{Y}_1, \mathbf{Y}, \mathbf{Y}_2)$. The insight behind is that, if we update D_2 by always expecting that the distance between \mathbf{Y}_2 and \mathbf{Y} is not small enough, then the generator G_2 is encouraged to produce \mathbf{Y}_2 closer to \mathbf{Y} and further from \mathbf{Y}_1 in the next iteration. By optimizing the ranking loss in such an adversarial manner, the Refine-Net is able to learn realistic dynamic patterns and generate vivid videos.

To better clarify the training procedure for Stage II, we present the key steps in Algorithm 1.

IV. EXPERIMENTS

A. Dataset

We build a relatively large-scale dataset of time-lapse videos from the Internet. By querying the key word of “Time-lapse” and “Sky” on the Youtube website, we are able to collect over 5,000 time-lapse videos. We manually cut these videos into short clips and select those containing dynamic sky scenes, such as the cloudy sky with moving clouds, and the starry sky with moving stars. Some of the clips may contain scenes that are kind of dark or contain effects of quick zoom-in and zoom-out, thus are abandoned.

We split the set of selected video clips into a training set and a testing set with a ratio of 9 : 1. Note that all the video clips belonging to the same long video are in the same set to ensure that there are no testing video clips that are associated in some way to those used in the training stage. We then decompose the short video clips into frames, and generate clips by sequentially combining continuous 32 frames as a clip. Note that there are no overlap between two

consecutive clips. By doing so, we collect 35,392 training video clips, and 2,815 testing video clips, each containing 32 frames. The original size of each frame is $3 \times 640 \times 360$, and we resize it into a square image of size 128×128 . Before feeding the clips to the model, we normalize the color values to $[-1, 1]$. No other preprocessing is required.

Our dataset is quite challenging. First, the content is complex. There are various types of scenes in the data set, including the daytime, the nightfall, the dawn, the starry night and the aurora. They exhibit different kinds of foreground (the sky), and colors. For instance, the scene of starry night contains stars, and the color of the scene is usually dark blue. The daytime scene is quite different as the major dynamics comes from the moving cloud, and the color of sky is much brighter. Unlike some previous time-lapse video datasets, e.g. [7], which contains relatively clean background, the background in our dataset shows high-level diversity across videos. The scenes may contain trees, mountains, buildings and other static objects. Second, the motion is diverse. The dynamic patterns within each type of scene differ from one another. The clouds in the sky may be of any arbitrary shape and move in any direction. In the starry night scene, the stars usually move fast along a curve. The diversity of motions brings additional challenges for the model to capture a definite dynamic pattern.

Our dataset can be used for various tasks on learning dynamic patterns, including unconditional video generation [4], video prediction [6], video classification [29], and dynamic texture synthesis [24]. In this paper, we use it for video prediction. The samples of our dataset are displayed in the supplementary materials.

B. Implementation Details

We first train the Base-Net in Stage I on our training set, and then train the Refine-Net in Stage II based on the results from Stage I. Once the model is well trained, given one starting frame, we generate 32 frames of resolution 128×128 in a single forward pass, expecting the latter 31 frames as the future prediction of the first frame. The models in

Table I
THE ARCHITECTURE OF THE GENERATORS IN BOTH STAGES. THE SIZE OF THE INPUT VIDEO IS $3 \times 32 \times 128 \times 128$.

Layers	conv1	conv2	conv3	conv4	conv5	conv6	deconv1	deconv2	deconv3	deconv4	deconv5	deconv6
# Filters	32	64	128	256	512	512	512	256	128	64	32	3
Filter Size	(3, 4, 4)	(4, 4, 4)	(4, 4, 4)	(4, 4, 4)	(4, 4, 4)	(2, 4, 4)	(4, 4, 4)	(4, 4, 4)	(4, 4, 4)	(4, 4, 4)	(4, 4, 4)	(3, 4, 4)
Stride	(1, 2, 2)	(2, 2, 2)	(2, 2, 2)	(2, 2, 2)	(2, 2, 2)	(1, 1, 1)	(1, 1, 1)	(2, 2, 2)	(2, 2, 2)	(2, 2, 2)	(2, 2, 2)	(1, 2, 2)
Padding	(1, 1, 1)	(1, 1, 1)	(1, 1, 1)	(1, 1, 1)	(1, 1, 1)	(0, 0, 0)	(0, 0, 0)	(1, 1, 1)	(1, 1, 1)	(1, 1, 1)	(1, 1, 1)	(1, 1, 1)

Table II

QUANTITATIVE COMPARISON RESULTS OF DIFFERENT MODELS. WE SHOW PAIRS OF VIDEOS TO A FEW WORKERS, AND ASK THEM “WHICH IS MORE REALISTIC”. WE COUNT THEIR EVALUATION RESULTS, WHICH ARE DENOTED AS PREFERENCE OPINION SCORE (POS). THE VALUE RANGE OF POS COULD BE $[0, 100]$. IF THE VALUE IS GREATER THAN 50 THEN IT MEANS THE FORMER PERFORMS BETTER THAN THE LATTER.

“Which is more realistic?”	POS
Random Selection	50
Prefers Ours over VGAN	92
Prefers Ours over RNN-GAN	97
Prefers VGAN over Real	5
Prefers RNN-GAN over Real	1
Prefers Ours over Real	16

both stages are optimized with mini-batch stochastic gradient descent. We use Adam as the optimizer with $\beta = 0.5$ and the momentum is 0.9. The learning rate is set to 0.0002 and fixed throughout the training procedure. We use a batch size of 64 for the Base-Net and 32 for the Refine-Net.

We use Batch Normalization [30] followed by Leaky ReLU [31] in almost all the 3D convolutional layers in both the encoder part of generators and discriminators, except for their first and last layers. For the deconvolutional layers, we use ReLU [32] instead of Leaky ReLU. We use Tanh as the activation function of the output layers of the generators. The Gram matrices are calculated using the features of the first and third convolutional layers (after the ReLU layer) of discriminator D_2 . The weight of the adversarial ranking loss is set to 1 in all experiments, i.e., $\lambda = 1$. The detailed configurations of G_1 are given in Table I. The generator of the Refine-Net has quite similar structures with G_1 , except that we remove the skip-connections between “conv1” and “deconv6”, “conv2” and “deconv5”. The skip-connection is implemented by element-wisely summing the features of two layers [8]. No concatenation of layers is used. We train our model with four Tesla M40 GPUs.

C. Comparison with Existing Methods

We perform quantitative comparison between our model and the models presented in [4] and [7]. For notation convenience, we name these two models as VGAN [4] and RNN-GAN [7], respectively. For a fair comparison, we reproduce the results of their models exactly according to their papers and reference codes, except some adaption to match the same experimental setting as ours. The adaption

includes that, all the methods produce 32 frames as the output. Note that, both VGAN and RNN-GAN generate videos of resolution 64×64 , thus we resize the videos produced by our model to resolution 64×64 for fairness.

There has not been a proper metric for the objective evaluation of authenticity of generated videos, thus we use the same evaluation metric as in VGAN. Specifically, we compare the models in pairs. For each two models, we randomly select 100 clips from the testing set and take their first frames as the input. Then we produce the future prediction as a video of 32 frames by the two models. We conduct 100 times of opinion test based on the outputs. Each time we show a worker two videos generated from the two models given the same input frame. The worker is required to give opinion about which one is more realistic. The two videos are shown in a random order to avoid the potential issue that the worker tends to always prefer a video on the left (or right) due to laziness. Five groups of comparison are conducted in total. Apart from the comparisons between ours and VGAN and RNN-GAN, respectively, we also conduct comparison of ours, VGAN and RNN-GAN against real videos to evaluate the performance of these models.

Table II shows the quantitative comparison results. Our model outperforms VGAN [4] with regard to the Preference Opinion Score (POS). Qualitatively, videos generated by VGAN are usually not as sharp as ours. The following reasons are suspected to contribute to the superiority of our model. First, we adopt the U-net like structure instead of a vanilla encoder-decoder structure in VGAN. The connections between the encoder and the decoder bring more powerful representations, thus producing more concrete contents. Second, the Refine-Net makes further efforts to learn more vivid dynamic patterns. Our model also performs better than RNN-GAN [7]. One reason might be that RNN-GAN uses an RNN to sequentially generate image frames, thus their results are prone to error accumulation. Our model employs 3D convolutions instead of RNN so that the state of the next frame does not heavily depend on the state of previous frames.

When comparing ours, VGAN and RNN-GAN with real videos, our model consistently achieves better POS than both VGAN and RNN-GAN, showing the superiority of our multi-stage model. Some results of our model are indistinguishable from the real ones, or even perceived as more realistic than the real ones, suggesting that our model

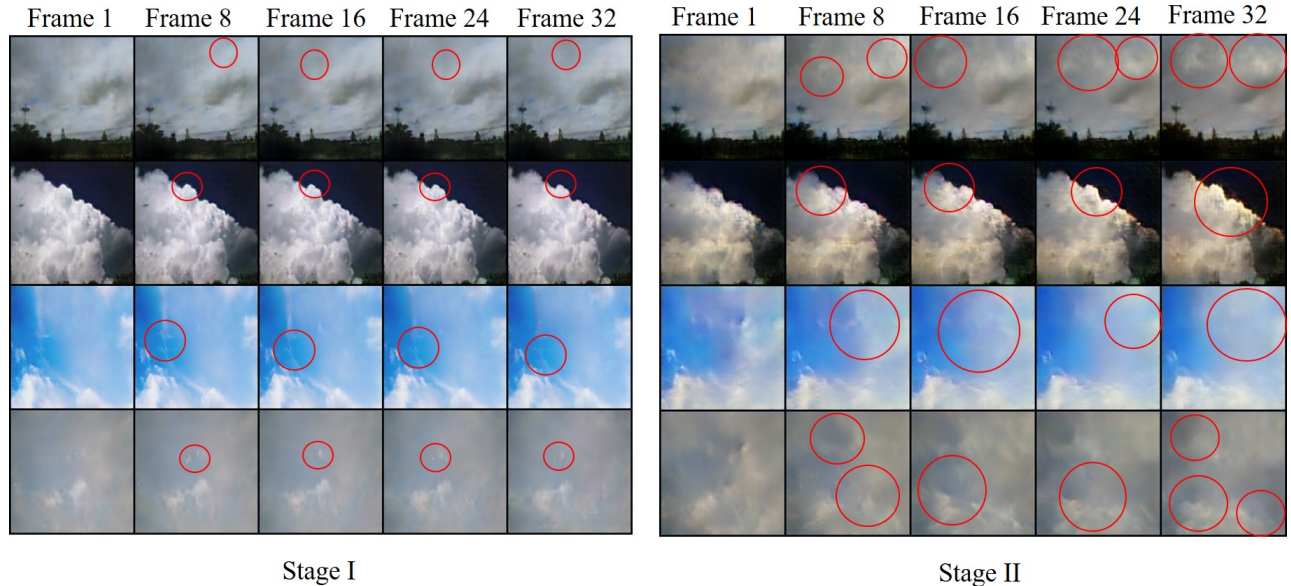


Figure 3. The generated video frames by Stage I (left) and Stage II (right) given the same first frame. We show exemplar frames 1, 8, 16, 24, and 32. Red circles are used to indicate the locations and areas where obvious movements take place between adjacent frames. Larger and more circles are observed in the frames of Stage II, indicating that there are more vivid motions generated by the Refine-Net. Best viewed in color.

is able to generate realistic and plausible future scenes.

D. Comparison between Base-Net and Refine-Net

Although the Base-Net can generate videos of decent details and plausible motion, it fails to generate vivid dynamics. For instance, some of the results in the scene of cloudy daytime fail to exhibit apparent cloud movement. The Refine-Net makes attempts to compensate for the motion and learns visual dynamics from data automatically. In this part, we evaluate the performance of Stage II versus Stage I in terms of both quantitative and qualitative results.

Quantitative Results. Given the same starting image as input, we generate two videos by the Base-Net in Stage I and the Refine-Net in Stage II separately. The comparison is carried out over 100 pairs of generated videos in a similar way as that in the previous section. Showing each pair of two videos, we ask the workers which one is more realistic. To check how effective our model is, we also compare the results of the Base-Net and Refine-Net with the groundtruth videos.

The results shown in Table III reveal that the Refine-Net contributes significantly to the realism of the generated

videos. When comparing the Refine-Net with the Base-Net, the advantage is about 40 (70 versus 30) in terms of the POS. Not surprisingly, the Refine-Net gains better POS than the Base-Net when comparing videos of these two models with the ground-truth videos.

Qualitative Results. We further compare the results of these two stages by diving into the details of each frame. To this end, we show four video clips generated by the Base-Net and the Refine-Net individually on the basis of the same starting frame in Fig. 3. Motions are indicated by red circles in the frames. Please note the differences between the next and previous frames. We also encourage the readers to check more qualitative results in our supplementary materials. Results in Fig. 3 indicate that although the Base-Net can generate concrete object details, the content of the next frames seems to have no significant difference from the previous frames. While it does captures the motion patterns to some degree, like the color changes or some inconspicuous object movements, the Base-Net fails to generate vivid dynamic scene sequences. In contrast, the Refine-Net take the result of the Base-Net to produce more realistic motion dynamics learned from the dataset. As a result, the scene sequences show more evident movements between adjacent frames and the resulting videos are more indistinguishable from the real videos.

Table III
QUANTITATIVE COMPARISON RESULTS OF STAGE I VERSUS STAGE II.
THE EVALUATION METRIC IS THE SAME AS THAT IN TABLE II.

“Which is more realistic?”	POS
Random Selection	50
Prefers Stage II to Stage I	70
Prefers Stage II to Real	16
Prefers Stage I to Real	8

V. CONCLUSIONS

We present a multi-stage dynamic generative adversarial network that can generate realistic time-lapse videos of resolution as high as 128×128 . In the first stage, our model generates plausible motion and content patterns by our Base-

Net with a structure of 3D U-net like network as the generator. In the second stage, our Refine-Net improves the motion quality with an adversarial ranking loss. The ranking loss incorporates the Gram matrix, which can effectively model the motion patterns of a video. Experiments show that our model outperforms the state-of-the-art models and can generate videos which are almost indistinguishable from real videos in many cases.

REFERENCES

- [1] K.-H. Zeng, T.-H. Chen, C.-Y. Chuang, Y.-H. Liao, J. C. Niebles, and M. Sun, "Leveraging video descriptions to learn video question answering," in *AAAI Conference on Artificial Intelligence (AAAI)*, 2017, pp. 4334–4340.
- [2] P. Ruolo, "Dude, where's my robot?: A localization challenge for undergraduate robotics," in *AAAI Conference on Artificial Intelligence (AAAI)*, 2017, pp. 4798–4802.
- [3] C. Vondrick and A. Torralba, "Generating the future with adversarial transformers," in *IEEE Conference on Computer Vision and Pattern Recognition (CVPR)*, 2017.
- [4] C. Vondrick, H. Pirsiavash, and A. Torralba, "Generating videos with scene dynamics," in *Advances In Neural Information Processing Systems (NIPS)*, 2016, pp. 613–621.
- [5] M. Mathieu, C. Couprie, and Y. LeCun, "Deep multi-scale video prediction beyond mean square error," *arXiv preprint arXiv:1511.05440*, 2015.
- [6] R. Villegas, J. Yang, Y. Zou, S. Sohn, X. Lin, and H. Lee, "Learning to generate long-term future via hierarchical prediction," *International Conference on Machine Learning (ICML)*, 2017.
- [7] Y. Zhou and T. L. Berg, "Learning temporal transformations from time-lapse videos," in *European Conference on Computer Vision (ECCV)*. Springer, 2016, pp. 262–277.
- [8] K. He, X. Zhang, S. Ren, and J. Sun, "Identity mappings in deep residual networks," in *European Conference on Computer Vision (ECCV)*. Springer, 2016, pp. 630–645.
- [9] L. Gatys, A. S. Ecker, and M. Bethge, "Texture synthesis using convolutional neural networks," in *Advances In Neural Information Processing Systems (NIPS)*, 2015, pp. 262–270.
- [10] I. Goodfellow, J. Pouget-Abadie, M. Mirza, B. Xu, D. Warde-Farley, S. Ozair, A. Courville, and Y. Bengio, "Generative adversarial nets," in *Advances In Neural Information Processing Systems (NIPS)*, 2014, pp. 2672–2680.
- [11] M. Mirza and S. Osindero, "Conditional generative adversarial nets," *arXiv preprint arXiv:1411.1784*, 2014.
- [12] A. Radford, L. Metz, and S. Chintala, "Unsupervised representation learning with deep convolutional generative adversarial networks," *International Conference on Learning Representations (ICLR)*, 2016.
- [13] M. Arjovsky, S. Chintala, and L. Bottou, "Wasserstein generative adversarial networks," *International Conference on Machine Learning (ICML)*, 2017.
- [14] P. Isola, J.-Y. Zhu, T. Zhou, and A. A. Efros, "Image-to-image translation with conditional adversarial networks," *IEEE Conference on Computer Vision and Pattern Recognition (CVPR)*, 2017.
- [15] J.-Y. Zhu, T. Park, P. Isola, and A. A. Efros, "Unpaired image-to-image translation using cycle-consistent adversarial networks," *International Conference on Computer Vision (ICCV)*, 2017.
- [16] S. Reed, Z. Akata, X. Yan, L. Logeswaran, B. Schiele, and H. Lee, "Generative adversarial text to image synthesis," *International Conference on Learning Representations (ICLR)*, 2016.
- [17] H. Zhang, T. Xu, H. Li, S. Zhang, X. Huang, X. Wang, and D. Metaxas, "Stackgan: Text to photo-realistic image synthesis with stacked generative adversarial networks," *International Conference on Computer Vision (ICCV)*, 2017.
- [18] E. Denton, S. Chintala, A. Szlam, and R. Fergus, "Deep generative image models using a laplacian pyramid of adversarial networks," in *Advances In Neural Information Processing Systems (NIPS)*, 2015, pp. 1486–1494.
- [19] D. P. Kingma and M. Welling, "Auto-encoding variational bayes," *International Conference on Learning Representations (ICLR)*, 2014.
- [20] T. Xue, J. Wu, K. L. Bouman, and W. T. Freeman, "Visual dynamics: Probabilistic future frame synthesis via cross convolutional networks," in *Advances In Neural Information Processing Systems (NIPS)*, 2016.
- [21] R. Villegas, J. Yang, S. Hong, X. Lin, and H. Lee, "Decomposing motion and content for natural video sequence prediction," *International Conference on Machine Learning (ICML)*, vol. 1, no. 2, p. 7, 2017.
- [22] S. Tulyakov, M.-Y. Liu, X. Yang, and J. Kautz, "Mocogan: Decomposing motion and content for video generation," *arXiv preprint arXiv:1707.04993*, 2017.
- [23] O. Ronneberger, P. Fischer, and T. Brox, "U-net: Convolutional networks for biomedical image segmentation," in *International Conference on Medical Image Computing and Computer-Assisted Intervention*. Springer, 2015, pp. 234–241.
- [24] C. M. Funke, L. A. Gatys, A. S. Ecker, and M. Bethge, "Synthesising dynamic textures using convolutional neural networks," *arXiv preprint arXiv:1702.07006*, 2017.
- [25] M. Tesfaldet, M. A. Brubaker, and K. G. Derpanis, "Two-stream convolutional networks for dynamic texture synthesis," *arXiv preprint arXiv:1706.06982*, 2017.
- [26] K. Simonyan and A. Zisserman, "Very deep convolutional networks for large-scale image recognition," *International Conference on Learning Representations (ICLR)*, 2015.
- [27] E. Hoffer and N. Ailon, "Deep metric learning using triplet network," in *International Workshop on Similarity-Based Pattern Recognition*. Springer, 2015, pp. 84–92.
- [28] X. Liang, H. Zhang, and E. P. Xing, "Generative semantic manipulation with contrasting gan," *arXiv preprint arXiv:1708.00315*, 2017.
- [29] A. Karpathy, G. Toderici, S. Shetty, T. Leung, R. Sukthankar, and L. Fei-Fei, "Large-scale video classification with convolutional neural networks," in *IEEE Conference on Computer Vision and Pattern Recognition (CVPR)*, 2014, pp. 1725–1732.
- [30] S. Ioffe and C. Szegedy, "Batch normalization: Accelerating deep network training by reducing internal covariate shift," in *International Conference on Machine Learning (ICML)*, 2015, pp. 448–456.
- [31] B. Xu, N. Wang, T. Chen, and M. Li, "Empirical evaluation of rectified activations in convolutional network," *arXiv preprint arXiv:1505.00853*, 2015.
- [32] V. Nair and G. E. Hinton, "Rectified linear units improve restricted boltzmann machines," in *International Conference on Machine Learning (ICML)*, 2010, pp. 807–814.